# The sequential two photon dissociation of NO as a source of aligned N( 2D), N( 4S) and O( 3P) atoms

**ARTICLE** *in* CHEMICAL PHYSICS LETTERS · FEBRUARY 1998

Impact Factor: 1.9 · DOI: 10.1016/S0009-2614(97)01414-0



**6 AUTHORS**, INCLUDING:

David H Parker
Radboud University Nijmegen
**204** PUBLICATIONS **4,808** CITATIONS
SEE PROFILE

Grant A D Ritchie
University of Oxford
**107** PUBLICATIONS **1,074** CITATIONS
SEE PROFILE

13 February 1998

ELSEVIER

Chemical Physics Letters 283 (1998) 319–325

CHEMICAL PHYSICS LETTERS

# The sequential two photon dissociation of NO as a source of aligned $N(^2D)$, $N(^4S)$ and $O(^3P)$ atoms

Bernard L.G. Bakker [a], André T.J.B. Eppink [a], David H. Parker [a], Matthew L. Costen [b], Gus Hancock [b], Grant A.D. Ritchie [b]

[a] *Department of Molecular and Laser Physics, Catholic University of Nijmegen, NL 6525 Nijmegen, Netherlands*
[b] *Physical and Theoretical Chemistry Laboratory, Oxford University, South Parks Road, Oxford OX1 3QZ, UK*

Received 21 November 1997; in final form 8 December 1997

**Abstract**

Velocity map imaging is used to characterise the angular distributions of atoms which are formed from the sequential two photon excitation of NO via the $A^2\Sigma^+$ state. Molecules excited at 226 nm and dissociated at 339 nm from the same laser source yield two sets of products, ground state $O(^3P)$ atoms in conjunction with $N(^2D)$ and $N(^4S)$. The angular distributions are found to be well described by $\beta$ parameters. The use of this method as a source of monoenergetic aligned atoms for studies of reaction dynamics is discussed. © 1998 Elsevier Science B.V.

## 1. Introduction

One of the most significant developments in gas phase reaction dynamics over the past ten years has been in the use of laser prepared reagents to study the stereodynamics of chemical reactions. Polarised laser photolysis of a suitable precursor molecule forms a velocity aligned reagent (generally an atom) and measurements of the polarisation of its reaction products probed by laser induced fluorescence (LIF) or resonance enhanced multiphoton ionisation (REMPI) can give unprecedented detail about the quantum state resolved dynamics of the reaction [1–3]. When a diatomic molecule is used as the precursor, then photolysis produces an essentially monoenergetic reagent distribution, as for example in studies of the reactions of H and Cl atoms formed by photolysis of HI [4,5], HBr [6] and $Cl_2$ [7]. In contrast, reactions of oxygen atoms have relied on the photolysis of the triatomic precursors $N_2O$ [8,9] and $O_3$ [10] for $O(^1D)$, and $NO_2$ [11,12] for $O(^3P)$ and this necessarily complicates the interpretation of the measured polarisations, as the atomic reagent now has a range of kinetic energies and possibly a speed dependent anisotropy.

Here we describe a straightforward method of producing aligned nitrogen and oxygen atoms by the sequential two photon dissociation of NO via the $A^2\Sigma^+$ state. We form monochromatic $N(^2D)$ atoms in conjunction with ground state $O(^3P)$ and observe a second channel forming fast ground state O and N atoms. In this Letter we concentrate on the translational anisotropy of the $N(^2D) + O(^3P)$ channel measured by velocity map imaging of both frag-


*PII* S0009-2614(97)01414-0

ments [13] and discuss the use of this method as a strategy of studying the reactions of monoenergetic velocity aligned N and O atoms.

## 2. Experimental

The velocity mapping apparatus, a variant of ion imaging [14] has been described in detail before [13,15] and is summarised here. A pulsed supersonic beam of 20% NO in He (1 bar) is directed down the axis of a time-of-flight (TOF) mass spectrometer and crossed at right angles with the counterpropagating pulsed dye laser beams. The output of the first dye laser (678 nm) is both frequency doubled and tripled to produce radiation at 226 and 339 nm. These beams are separated and used, first to excite NO to the $A^2\Sigma^+$ state near 226 nm ($\sim 0.4$ mJ pulse$^{-1}$, irised to match the 1.2 mm diameter molecular beam), and then to dissociate by absorption at 339 nm ($\sim 2$ mJ pulse$^{-1}$ loosely focused to the same diameter).

Atomic products are ionised by REMPI, using the output of a second dye laser focused tightly on the molecular beam with a 20 cm lens. Three detection schemes were successfully used, for $N(^2D)$ at 269 nm [16], $O(^3P)$ at 226 nm [17] and $N(^4S)$ at 211 nm [18]. Less than 1 mJ pulse of the radiation (produced by frequency doubling) was required. The detection laser pulse arrived $\sim 20$ ns after the production pulse. In each case the detection laser wavelength was scanned repetitively across the transition's Doppler profile to ensure equal detectivity for all velocity groups.

Ions formed by REMPI were extracted from the ionisation region into the grounded time-of-flight tube and crushed onto a two-dimensional microchannel plate/phosphor screen detector read by a CCD camera. An electrostatic immersion lens [13] is used, which projects all ions with the same velocity to the same point on the 2D detector regardless of their position of origin in the ionisation volume, improving the velocity resolution compared to the use of grids in conventional ion imaging. Mass selectivity is achieved by pulsing the gain of the detector as the $N^+$ or $O^+$ ions arrive. Even without such pulsing, the residual gain is high enough to amplify the residual $NO^+$ signal, which is intense enough in some cases to appear in the middle of the image (no kinetic energy release) as a leakage signal. Typically 5000 laser shots were used to produce the final image, which was inverted (2D–3D) using a Hankel inversion programme.

## 3. Results

The NO A–X transition lies in a convenient range for laser excitation (around 226 nm for the 0–0 band [19]) and a large volume of molecules can be excited with unfocussed laser light. Dissociation of the excited molecules to form the aligned atoms should ideally be carried out with photons which are produced by the **same** laser but are normally unused. None of the pump YAG laser harmonics (532, 355 and 266 nm) were found to dissociate the NO A state to produce measurable atomic products. 452 nm radiation, available when producing the 226 nm light by frequency doubling was similarly unsuccessful. 339 nm radiation however, which comes ''free'' when 226 nm light is formed by frequency tripling, was found to be particularly efficient in producing energetic atoms.

Sequential two step dissociation of NO using (226 + 339) nm photons and detection of $N(^2D_{3/2})$ atoms using 269 nm photons yields the raw image shown in Fig. 1. In these experiments the A–X laser is set at $44197.5 \pm 2$ cm$^{-1}$ (226.19 nm) at the $Q_{11} + P_{21}$ bandhead, exciting predominantly the $N'' = 1$, 2 and 3 rotational states which form the majority of population in the cold molecular beam and producing $A^2\Sigma^+$ molecules with the same values of $N'$ ($\Delta N = 0$). The laser polarisations all lie parallel to the detector face and thus along the vertical axis of Fig. 1. Under these conditions, transformation of the 2D image to the original 3D pattern using the Hankel inversion is possible, and yields the angle integrated kinetic energy distribution shown in Fig. 2a. Calibration of the velocity and thus kinetic energy release of the atoms is based on the known properties of the inversion lens, which were checked against distributions previously measured for $O(^3P)$ detection from the photolysis of molecular oxygen [15].

Three features can be seen in Fig. 2a. At low kinetic energies there is a leakage signal, present when both the 339 and 269 nm laser beams are

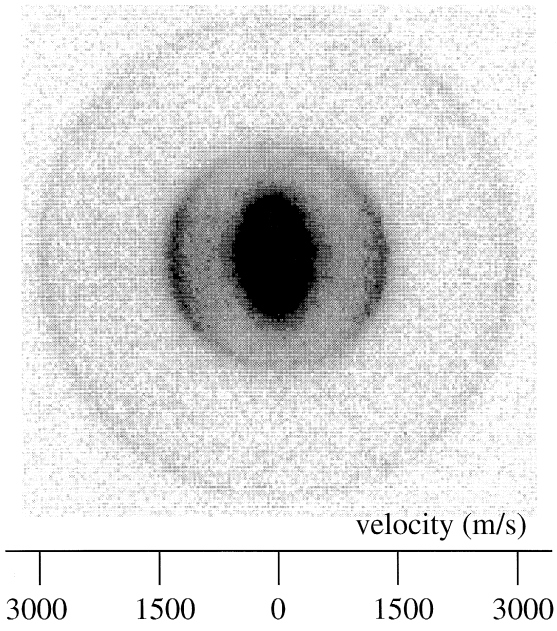


Fig. 1. Raw image of $N^+$ formed from $N(^2D_{3/2})$ by REMPI at 269 nm following the sequential two photon excitation of NO at 226 + 339 nm. The 339 nm beam polarisation vector is along the vertical axis of the figure. The asymmetric inner feature is from $NO^+$ leakage signal caused by 1 + 1 REMPI of the molecule at 226 nm. The pronounced feature at a velocity of 1400 $ms^{-1}$ can be clearly seen as arising from fragments travelling perpendicular to the polarisation vector: in addition a weak outer ring is observed.

blocked, which arises from $NO^+$ formed in the 1 + 1 REMPI of NO at 226 nm. An outer ring, with 0.66 eV kinetic energy, is also seen in the absence of 339 nm radiation, which is caused by dissociation of A state molecules by absorption of the 269 nm REMPI detection radiation. The major peak at 0.14 eV is at precisely the position expected for the sequential 226 + 339 nm steps forming $N(^2D)$ together with ground state $O(^3P)$.

Fig. 2b shows the angular distribution of the 0.14 eV peak. The maximum signal is seen at 90° to the laser beams' polarisation axis (as can clearly be seen in the image of Fig. 1) and when fitted to the equation $I(\theta) = 1 + \beta P_2(\cos\theta)$, where $P_2(\cos\theta)$ is the second order Legendre polynomial, yielded a value of $\beta = -0.8 \pm 0.05$. The errors represent a $1\sigma$ deviation from the results of 7 separate experiments. In the A–X transition, we are in principle forming aligned NO molecules and thus the angular distribution of the dissociation products should not be described by this simple expression. In practice the alignment is likely to be small for the following reasons. Excitation to the A state is in both Q and P branch transitions which have opposite polarisations relative to the angular momentum vector $\boldsymbol{J}$ and similar line strengths at low $N''$, and the dissociation step is from A state molecules whose alignment is reduced by rotation. Hyperfine depolarisation will also reduce the alignment in these low $N'$ levels. These effects are expected to wash out any alignment in the A–X excitation. This was experimentally confirmed by the invariance in the $\beta$ value found

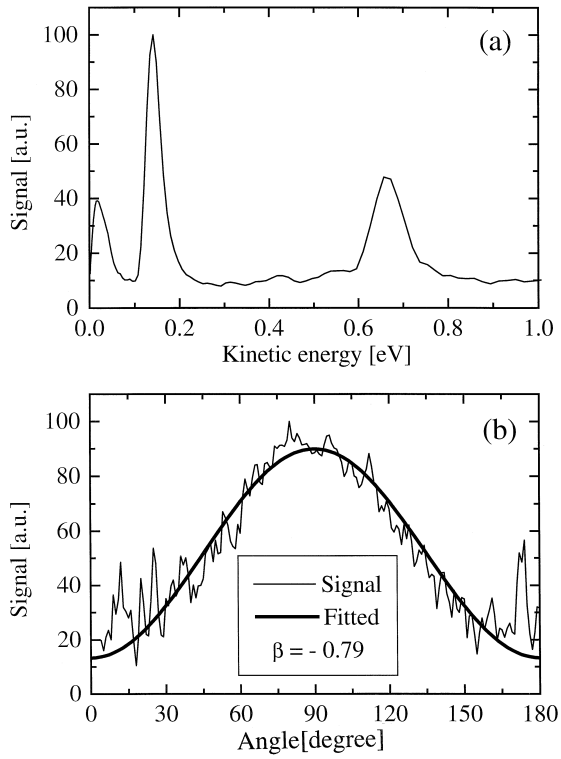


Fig. 2. Upper panel (a): angle integrated kinetic energy distribution of the $N(^2D_{3/2})$ fragment taken from the data of Fig. 1. The inner leakage signal from $NO^+$ gives rise to the feature at low kintetic energy (0.03 eV), the major peak at 0.14 eV is from sequential 226 + 339 nm dissociation of NO to give $N(^2D) + O(^3P)$ and the peak at 0.66 eV (the outer ring of Fig. 1) is from 226 + 269 nm absorption, the latter wavelength being that used to ionise $N(^2D)$. Lower panel (b): angular distribution of the 0.14 eV $N(^2D_{3/2})$ peak relative to the 339 nm laser polarisation vector. A perpendicular transition is seen, with the data fitted to yield a $\beta$ parameter of $-0.79$ for this data set.

when the polarisation vector of the 226 nm beam was rotated so that it was along the TOF axis. Incorporating a $P_4(\cos\theta)$ term in the angular distribution produced only marginally better fits. The detection step, 2 + 1 REMPI at 269 nm, can also be selective if atoms are formed with an anisotropic distribution of $m_J$ states and the absorption steps are polarisation dependent. This effect was shown to be insignificant by the invariance of the angular distributions on rotation of the 269 nm polarisation vector with respect to that of the dissociating 339 nm beam. Our results suggest that the angular distributions of $N(^2D)$ are well described by a single $\beta$ parameter, but we note that we have been unable to find evidence that the $m_J$ substates are aligned with respect to the atomic velocity vector. Experiments on the $N(^2D_{5/2})$ state produced the same images as for $N(^2D_{3/2})$.

Fig. 3 shows the raw image when $O(^3P_2)$ atoms were detected following 226 + 339 nm dissociation and the angle integrated kinetic energy distribution is shown in Fig. 4a. The ''inner ring'' at 0.13 eV is at the position expected for the $N(^2D) + O(^3P_2)$ channel and the angular distribution, an example of which

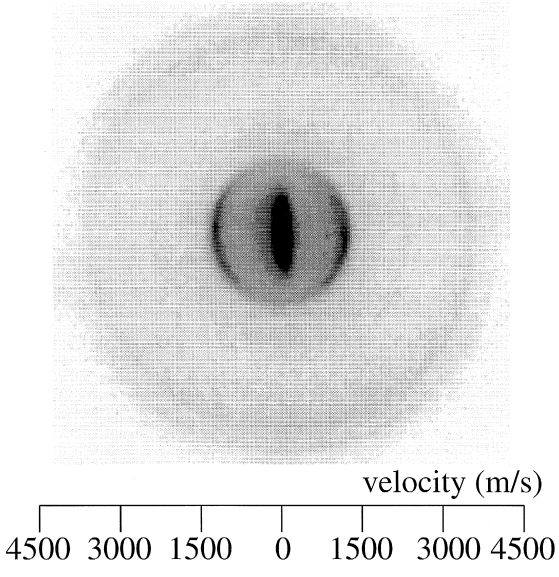


Fig. 3. Raw image of $O^+$ formed from $O(^3P_2)$ by REMPI at 225.7 nm following irradiation of NO at 226 + 339 nm. As in Fig. 1, the inner ''blob'' is caused by leakage signal from $NO^+$. The perpendicular transition giving O atoms with a velocity of 1250 $ms^{-1}$ is clearly seen, together with diffuse outer rings.

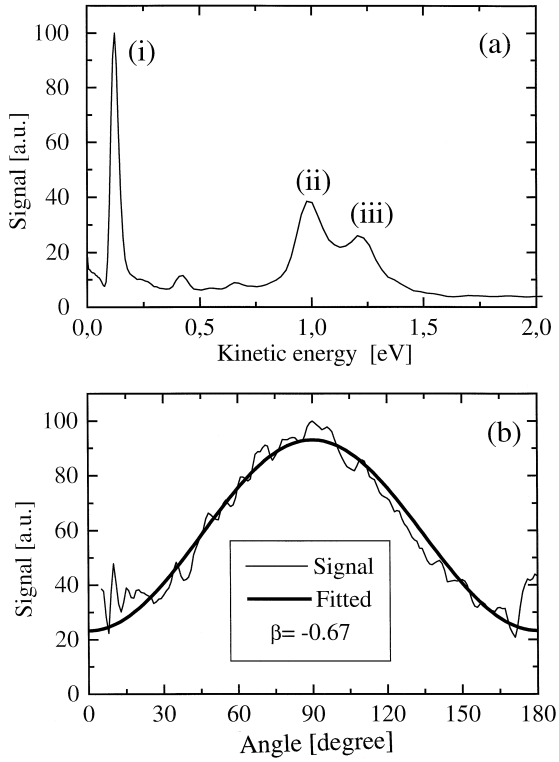


Fig. 4. Upper panel (a): angle integrated kinetic energy distribution of the $O(^3P_2)$ fragment taken from the data of Fig. 3. Feature (i) is from 226 + 339 nm sequential dissociation of NO, and is the O atom counterpart of the 0.14 eV peak seen in Fig. 2a. Feature (ii) at 0.94 eV is from 226 + 225.7 nm sequential two photon dissociation to give $N(^2D) + O(^3P)$ products, the 225.7 nm radiation both exciting the A state NO molecules and ionising the $O(^3P)$. The outer ring (iii) at 1.23 eV is from 226 + 339 nm dissociation forming ground state $N(^4S) + O(^3P)$ atoms. Lower panel (b): angular distribution of peak (i) in (a). A $\beta$ value of $-0.67$ was returned for this data set.

is shown in Fig. 4b, yields a value of $\beta = -0.71 \pm 0.17$ from the analysis of 23 separate images, in agreement with the $N(^2D)$ data. An outer ring at 1.23 eV is also seen, which corresponds to the formation of fast $O(^3P_2)$ together with ground state $N(^4S)$ atoms. Its polarisation is found to correspond to a parallel transition ( $\beta = 1.0 \pm 0.27$). The branching ratio for the channels $[O(^3P_2) + N(^4S)] : [O(^3P_2) + N(^2D)]$ was found to be $0.3 \pm 0.1$. In addition a $NO^+$ leakage signal (the central blob in Fig. 3) and an additional signal at 0.94 eV were seen in the absence of 339 nm light. Both signals are caused by the $O(^3P_2)$ detection laser set at 225.7 nm, which can

either ionise the A state molecules or dissociate them to form the $N(^2D)$ product. Both of these signals are unavoidable with $O(^3P_2)$ detection, but would be absent in a photolysis experiment. The angular distributions of the signals caused by the detection laser and the dynamics of the channel forming ground state products will be described in a future publication [20]. Detection of $O(^3P_1)$ and $O(^3P_0)$ requires wavelengths which are more closely resonant with NO A–X transitions in the molecular beam. The resultant high density of $NO^+$ ions (from $1+1$ REMPI) yielded space charge effects which precluded taking meaningful images for these two states.

Detection of $N(^4S)$ atoms by REMPI at 211 nm showed a strong feature corresponding to the $N(^4S) + O(^3P)$ channel with a $\beta$ value agreeing, within experimental error, with that found for the ''outer ring'' in Fig. 4. No evidence of a channel forming $O(^1D) + N(^4S)$ was seen both in these experiments and in attempts to observe $O(^1D)$ directly by REMPI.

## 4. Discussion

A schematic potential energy diagram of the relevant NO electronic states and their dissociation limits is shown in Fig. 5. The absorption of 339 nm light by A state NO brings the molecule to a total energy of 9.14 eV, which is below the ionisation potential, 0.26 eV above the $N(^2D) + O(^3P)$ dissociation limit, 0.67 eV above the $O(^1D) + N(^4S)$ limit and 2.64 eV above the $N(^4S) + O(^3P)$ limit. The (spin forbidden) $O(^1D) + N(^4S)$ channel is found to be inactive. Conservation of momentum and energy predicts the production of $N(^2D)$ atoms with 0.14 eV kinetic energy and $O(^3P)$ atoms with 1.23 and 0.13 eV kinetic energy, in agreement with the observed values.

Photodissociation properties of NO excited below the ionisation potential have been reported in several studies. Slanger et al. [21] were the first to show that NO predissociates following simultaneous two-photon excitation around 270 nm to high vibrational levels of the $n\mathrm{d}\pi$ Rydberg states, forming $N(^2D)$ atoms. Umemoto and Matsumoto [22] showed that two photon excitation at 275.3 nm is an efficient method of forming $N(^2D)$, and this has been used as a source of the atom in studies of the $N(^2D) + H_2$ reaction [23]. The main dissociation channel of the $n\mathrm{p}\pi$ Rydberg states appears to be predissociation via the repulsive wall of the bound $L^2\Pi$ valence state (see Fig. 5) [24]. Direct dissociation via repulsive valence states or via the repulsive wall of bound valence states has not been indicated in previous studies and the present lack of signals at non-resonant wavelength agrees with this.

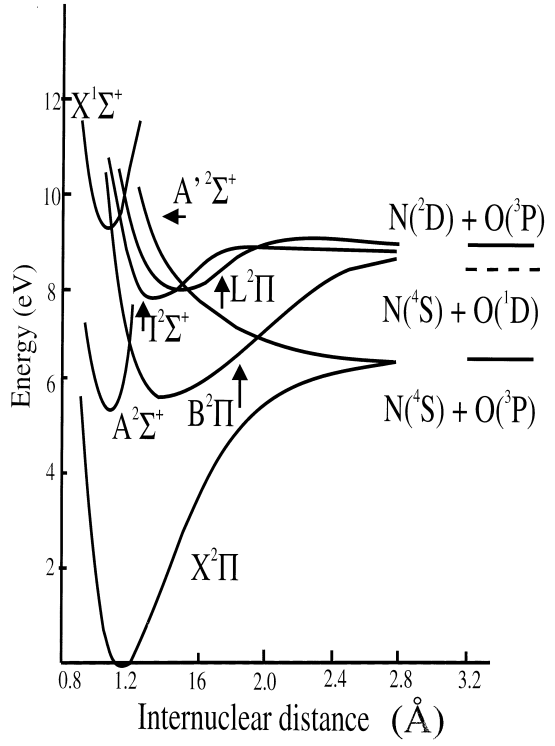


Fig. 5. Potential energy curves for NO, showing the positions of the dissociation limits and of the valence curves correlating with them.

Photoexcitation of low rotational levels of the $A^2\Sigma^+$ ($v = 0$) state by 335–345 nm photons has been reported by Fujii and Morita [25–27] and more recently by Geng et al. [28]. These studies and the earlier work of Anezaki et al. [29] have shown that two Rydberg states, the 11p($v = 0$) and the 10f($v = 0$), lie in this region. In the present experiment the second photon is at 29465 $cm^{-1}$ and is near (but not exactly resonant with) transitions from $N' = 2$ of the A state to the sublevels of the 11p complex which were observed by Geng et al. [28]. The photon energy, however, is resonant with an allowed (but

apparently weak [28]) P branch transition from $N' = 3$ in the A state to $N = 2$ in the $^2\Pi^+$ component of the 11p Rydberg state and we note that $N' = 3$ is populated following absorption at 226.19 nm. The 11p $^2\Pi$ levels are known to be broadened by predissociation through coupling to the L valence state continuum [24,28] or the repulsive part of the B valence state [28], both of which lead to $N(^2D) + O(^3P)$ products. The excitation process is thus $11p^2\Pi \leftarrow A^2\Sigma^+$ and should give a perpendicular transition ( $\beta < 0$), as observed. Furthermore, we can expect a reduction of the magnitude of the anisotropy parameter $\beta$ from its limiting value because of the Rydberg state lifetime. A change of $\beta$ from $-1$ to $-0.75$ (the average of the measurements on the $N(^2D)$ and $O(^3P)$ channels) would be consistent with the $^2\Pi^+$ $N = 2$ rotational level having a lifetime of 350 fs, which would result in a 15 $cm^{-1}$ linewidth. Geng et al. observed a linewidth of $\sim 5$ $cm^{-1}$ for the $N = 3$ level of this state [28]: we note that our estimate of the linewidth from the $\beta$ value depends upon the rotational frequency used in the Rydberg level and hence upon the value of $N$.

The predissociation mechanism for the channel forming $N(^4S) + O(^3P)$ in a parallel transition is less straightforward, but may be accounted for by absorption to a $^2\Sigma$ component of either the 11p or 10f Rydberg states: current experiments in which the excitation wavelength and laser power near 339 nm will be independently varied are aimed at unravelling the dissociation dynamics in this region.

## 5. A strategy for hot atom production

The cross section for excitation of the 11p Rydberg state from the NO A state has been estimated as $2.5 \times 10^{-18}$ $cm^2$ [25] and thus with presently available laser powers a volume of aligned atoms similar to that formed in single photon dissociation processes can be produced. This should enable full vector correlations to be measured for reactions of highly aligned $N(^2D)$ atoms: the method has an advantage over the two photon excitation process near 275 nm [22,23] in that a focused laser beam must be used in the latter process. This step appears to produce essentially velocity unaligned $N(^2D)$ atoms and also a substantial and wavelength dependent contribution from the channel forming hot ground state atomic products [20]. For $O(^3P)$ atoms the present method is not ideal, forming as it does, two sets of monochromatic atoms with opposite values of $\beta$. It points the way, however, to a future strategy involving predissociation of other Rydberg states which lie below dissociation limits other than to ground state atoms, but which can only be reached if a separately tunable laser source is available. Highly translationally excited $O(^3P)$ atoms can be formed, thus overcoming the energy barriers which are generally associated with this atomic reactant: an additional bonus is that fast $N(^4S)$ can also be produced.

One potential problem in the method will be seen if LIF is used as the probe for the reactions of such aligned atoms — strong emission from the NO A state will always be present as a background signal. However, if REMPI detection is used this problem disappears and a further advantage is gained, in that co-expansion of the NO precursor with the reagent will lead, as in the present study, to population in only a small number of rotational levels and thus enable a high proportion of the ground state molecules to be excited. Such studies are currently underway in our laboratory.

## Acknowledgements

The work in Nijmegen is part of the program of the Foundation Fundamental Research on Matter (FOM) and was made possible by financial support from The Netherlands Organisation of Science (NWO). We are grateful to the British Council for a travel grant.

## References

[1] A.J. Orr-Ewing, R.N. Zare, in: K. Liu, A.L. Wagner (Eds.), Chemical Dynamics of Small Free Radicals, World Scientific, Singapore, 1995.
[2] M. Brouard, J.P. Simons, in: K. Liu, A.L. Wagner (Eds.), Chemical Dynamics of Small Free Radicals, World Scientific, Singapore, 1995.
[3] A.J. Orr-Ewing, J. Chem. Soc. Faraday Trans. 92 (1996) 881.
[4] N.E. Shafer, H. Xu, R.P. Tuckett, M. Springer, R.N. Zare, J. Phys. Chem. 98 (1994) 3369.

[5] R. Fei, X.S. Zheng, G.E. Hall, J. Phys. Chem. 101 (1997) 2541.
[6] M. Brouard, H.M. Lambert, S.P. Rayner, J.P. Simons, Mol. Phys. 89 (1996) 403.
[7] W.R. Simpson, A.J. Orr-Ewing, R.N. Zare, Chem. Phys. Lett. 212 (1993) 163.
[8] M. Brouard, H.M. Lambert, J. Short, J.P. Simons, J. Phys. Chem. 99 (1995) 13571.
[9] A.J. Alexander, M. Brouard, S.P. Rayner, J.P. Simons, Chem. Phys. 207 (1996) 215.
[10] D.S. King, D.G. Sauder, M.P. Casassa, J. Chem. Phys. 97 (1992) 8919.
[11] F. Green, G. Hancock, A.J. Orr-Ewing, Faraday Discuss. Chem. Soc. 91 (1991) 79.
[12] M.L. Costen, G. Hancock, A.J. Orr-Ewing, D. Summerfield, J. Chem. Phys. 100 (1994) 2754.
[13] A.T.J.B. Eppink, D.H. Parker, Rev. Sci. Instrum. 68 (1997) 3477.
[14] A.J.R. Heck, D.W. Chandler, Annu. Rev. Phys. Chem. 46 (1995) 335.
[15] D.H. Parker, A.T.J.B. Eppink, J. Chem. Phys. 107 (1997) 2357.
[16] G. Black, L.E. Jusinski, Chem. Phys. Lett. 1339 (1987) 41.
[17] D.J. Bamford, L.E. Jusinski, W.K. Bischel, Phys. Rev. A 26 (1987) 3497.
[18] C.P. Fell, J.I. Steinfeld, S.M. Miller, Spectrochem. Acta 46 A (1990) 431.
[19] E. Meischer, F. Alberti, J. Phys. Chem. Ref. Data 5 (1976) 309.
[20] B.L.G. Bakker, A.T.J.B. Eppink, D.H. Parker, to be published.
[21] L.E. Jusinski, G.E. Gadd, G. Black, T.G. Slanger, J. Chem. Phys. 90 (1989) 4282.
[22] H. Umemoto, K. Matsumoto, J. Chem. Soc. Faraday Trans. 92 (1996) 1315.
[23] H. Umemoto, T. Asai, Y. Kimura, J. Chem. Phys. 106 (1997) 4985.
[24] A. Giusti-Suzor, Ch. Jungen, J. Chem. Phys. 80 (1984) 986.
[25] A. Fujii, N. Morita, Chem. Phys. Lett. 182 (1991) 304.
[26] A. Fujii, N. Morita, J. Chem. Phys. 97 (1992) 327.
[27] A. Fujii, N. Morita, Laser Chem. 13 (1994) 259.
[28] J. Geng, T. Kobayashi, M. Takami, Chem. Phys. Lett. 226 (1997) 290.
[29] Y. Anezaki, T. Ebata, N. Mikami, M. Ito, Chem. Phys. 97 (1985) 153.